Ergodicity breaking of an inorganic glass aging near T_g probed by elasticity relaxation

Xu Wang,[1,*] Jianbiao Wang,[2,†] and Haihui Ruan[3]

[1]*Ministry of Education Key Laboratory of Impact and Safety Engineering, Ningbo University, Ningbo, Zhejiang Province 315211, China*
[2]*Biel Crystal(Huizhou) Limited Company, Qiuchang Baishi Villige, Huiyang District, Huizhou, Guangdong Province 516227, China*
[3]*Department of Mechanical Engineering, The Hong Kong Polytechnic University, Hung Hum, Kowloon, Hong Kong, China*

(Received 9 October 2022; accepted 12 January 2023; published 30 January 2023)

We performed a series of aging experiments with an inorganic glass (As_2Se_3) at a temperature T_2 near the glass transition point T_g by first relaxing it at T_1. The relaxations of Young's modulus were monitored, which were (almost if not ideally) exponential with T_1-dependent relaxation time τ, corroborating the Kovacs' paradox in an inorganic glass. Associated with the divergence of τ, the quasiequilibrated Young's modulus E_∞ does not converge either. An elastic model of relaxation time and a Mori-Tanaka analysis of E_∞ lead to a similar estimate of the persistent memory of the history, illuminating ergodicity breaking within the accessible experimental time, as described in the Gardner transition theory. Experiments with different T_2 exhibit a critical temperature $T_p \sim T_g$, i.e., when $T_2 > T_p$, both τ and E_∞ converge. The results unveil a long-expected phenomenon that structural glass transition could be a zero-to-nonzero transition, manifested by a nonvanishing structural memory in aging when the temperature is below T_p in the glass transition range. This demonstrates the existence of the ergodicity breaking deep in the glass state and T_p could be the Gardner transition point of the structural glass.

DOI: 10.1103/PhysRevB.107.024205

I. INTRODUCTION

The microscopic dynamic behaviors of an amorphous system and the corresponding complex free-energy landscape is a high-profile and challenging subject in theoretical physics and material science [1,2]. Aging experiments of the spin glass [3] revealed a nonvanishing dependence on historic disturbance especially when it was applied with a long waiting time. This was manifested by not only the varied spectrum of relaxation time, but also the nonconverged physical quantity in an experimentally accessible duration [4]. Such observations together with the similar results of numerical simulations [5,6] have led to the concept of ergodicity breaking (EB) described by a phenomenological model based on a rugged free-energy surface, or more analytically, replica symmetry breaking (RSB), revealed in the mean-field solutions of spin systems [2,7]. In 2021, Giorgio Parisi was awarded the Nobel Prize in physics due to the exact solution of the mean-field spin glass transition [8–10]. In spin glass, the EB manifested as the divergence of magnetic susceptibility when specimens are cooled along different paths in the temperature-magnetic field with the same start and end points. The typical paths are called zero-field cooling (ZFC) and field cooling (FC), leading to different magnetic susceptibilities below a transition temperature.

As it is generally believed that the results of spin glass can be extended to structural glasses due to the amorphous state, revealing that the EB phenomenon in structural glasses becomes interesting and important. In 1985, Gardner [11] introduced a further development of the random first order transition (RFOT) [12] that occurs when the deep basins of a free energy landscape can split into fractal and hierarchical subbasins, corresponding to a marginally stable state of the system. This process occurs when the system is compressed or cooled beyond a threshold, and is defined as the Gardner transition. This impalpable transition is realized theoretically in a finite-dimensional system [13–15], while for the real system in which $d = 2$ or 3, the extrapolation and continuity of the solution must be checked. In 2017, Jin and Yoshino [16] explored the complex structure of the free-energy landscape of the simplest glass through the hard sphere system. They designed laboratory-reproducible rheological protocols to examine the dynamic features of the hard sphere system, in which compressing first then shearing corresponds to the ZFC protocol, and shearing followed by compression is regarded as the FC protocol. They found that shear modulus showed a protocol dependence when the density, or the pressure, reaches a critical value. Through the MD simulation, the trajectories of the spheres were tracked, which shows the aging behavior after the shear modulus bifurcates, displaying the EB phenomenon visually. The Gardner transition is examined in this three-dimensional hard sphere system, and the split point of the modulus is defined as the transition point. However, it is still arguable on the possibility of finding any EB phenomenon in real structural glass, considering that the built-in randomness of spin-spin interactions differs fundamentally from the self-generated position randomness in structural glass. Kovacs' experimental study on the volume relaxation of a polymeric glass below T_g in 1964 [17] challenged the ergodicity of the glassy system. The experiments show that the effective relaxation time (τ_{eff}) after long-time aging was still affected by the initial state especially in the experiments of temperature up jump. Because of the presumed uniqueness of an equilibrium (ergodic) state (note that the equilibrated volume was not provided by Kovacs [17]), the observed

*Corresponding author: wangxu@nbu.edu.cn
†Corresponding author: wangjb.vip@outlook.com

divergence of τ_{eff} was termed as "expansion-gap paradox" or "τ_{eff} paradox" [18,19], questioning how a quasiequilibrated system can exhibit disparate dynamics. Owing to the fundamentality in understanding glass relaxation, Kovacs' experiment was later reexamined by McKenna *et al.* [18] and repeated by Koll and Simon [19], which confirmed the gap in the quasiequilibrium τ_{eff}. Kovacs' finding of the expansion gap seemingly hints at the possibility. However, his results were criticized especially by the inorganic glass community [20–22] as the dilatometry experiments with inorganic glasses [23,24] after Kovacs did not render a convincing trend of persistent history dependence near T_g. For example, Goldstein and Nakonecznyj [23] speculated that the τ_{eff} paradox might not be found in inorganic glasses because they had a narrower relaxation-time spectrum than a polymeric glass did. Struik [25] criticized that the τ_{eff} paradox might merely be a manifestation of the divergence of τ_{eff} when a stretched exponential process approached equilibrium. These criticisms might have discouraged the effort following the route of Kovacs to unveil an EB phenomenon or the nature of glass transition in structural glasses through monitoring volume (V) change.

In this work, we switched our attention to the variation of Young's modulus (E) of a structural glass, as the Gardner transition in the hard sphere system displays. The Young's modulus is a two-time quantity (i.e., the autocorrelation function of stress or strain [26,27]) that can be analogous to the magnetic susceptibility of a spin glass and must be more sensitive to the heterogeneous dynamics in a glass [28]. Also, in experiments with structural glasses, E changes much more significantly in the temperature range of glass transition. Roughly speaking, $-lg(dE/dT/E)$ is 2–3 [29,30] and $-lg(dV/dT/V)$ is 5–6 [29] for an inorganic glass, i.e., the variation in Young's modulus is at least two orders of magnitude more significant than that in volume at temperatures near T_g. Hence, it is more plausible to probe an EB phenomenon, if any, based on $E(t)$ than that based on $V(t)$. Hereunder, we reported aging experiments with an inorganic glass, in which the relaxations of E were exponential. The exponentiality thus allows an undoubtful quantification of relaxation time τ as well as a clear quasiequilibrium magnitude of E_∞ when the aging time t is much larger than τ. Most unexpectedly, we show that both τ and E_∞ depend identically on thermal history, i.e., they do not converge at low temperatures but converge at high temperatures. It should be noted that for crystalline materials thermal history decides microstructures, which leads to different mechanical properties. For amorphous materials, such a history dependence occurs when the atomic arrangement is frozen. However, people often believe that structural relaxation—if it occurs at an elevated temperature close to T_g—should lead to the converged mechanical properties. In this work, we challenge this common understanding based on experimental results, i.e., we demonstrate that EB, as revealed in spin glass and theoretical glass models, does occur in a structural glass transition.

II. MATERIALS AND METHODS

A. Sample preparation

The commercial chalcogenide glass As_2Se_3 (Hubei New Hua-Guang Information Materials Co., Ltd, China) with the dilatometry $T_g = 180\,^\circ$C (at which the viscosity is approximately 1012 Pa s [31]) is chosen. As_2Se_3 glass is representative of chalcogenide glasses which has been widely used in infrared imaging [32] and optical switches [33]. It has excellent thermal stability against crystallization [34] with the lowest crystallization temperature of 200 °C, as extrapolated in the plot of isothermal crystallization rate [35]. The results presented in this paper were obtained from a sample of $40.025 \times 8.035 \times 2.45$ mm^3 and 3.6396 g, measured using impulse excitation technique (IET) station HT1600 (IMCE, Belgium).

B. Impulse excitation technique (IET)

The natural vibration of a beam generates sound, of which the frequency and attenuation reflect the viscoelastic properties of materials. for studying the temperature effect, the beam can be heated in a dedicated IET furnace (as shown in Fig. 1), into which argon gas is continuously purged to minimize the effect of oxidation. The samples in the device are fixed at the stationary (nodal) points of the first-order flexible vibration mode of a free-free beam, and hit at the middle span. A sound collection device is arranged above the midpoint of the sample. This collection device consists of a ceramic bar for transmitting the sound and a high-precision microphone for recording the sound signal. The Young's modulus, which is proportional to the square of frequency, is calculated according to the American Society for Testing and Materials (ASTM) standard 1876 [36] and the amplitude decay rate is determined from the full width at half maximum (FWHM) of the signal. This technique has been employed to study relaxation phenomena in various glasses [29,30,37–39] as well as the transient amorphous states during a crystalline phase transition [40].

C. Experimental protocol

Different from the ZFC and FC paths employed in spin glasses and the hard-sphere systems, here the path dependence, signifying the Gardner transition (or EB), is realized by the change in initial states. In experiments, the sample was first heated to and annealed at an initial temperature T_1 for a sufficiently long time to reach a quasiequilibrium state (no apparent trend of modulus change) and then quickly (about 0.5 °C/s) heated or cooled to the end temperature T_2. We chose[1] the commercial chalcogenide glass As_2Se_3. During heating, argon gas was purged to protect the sample from oxidation and Young's moduli were measured and recorded every 20 s.

[1]Several oxide glasses were attempted, but the results were much more contaminated by experimental fluctuations, causing ambiguity to make any judgement. A plausible cause could be the noise in high-temperature measurements because of the higher T_g (∼500 °C). The IET system we employed is to record the sound generated by sample vibration. At a higher temperature, the environmental noise further deteriorates the weak acoustic signal.

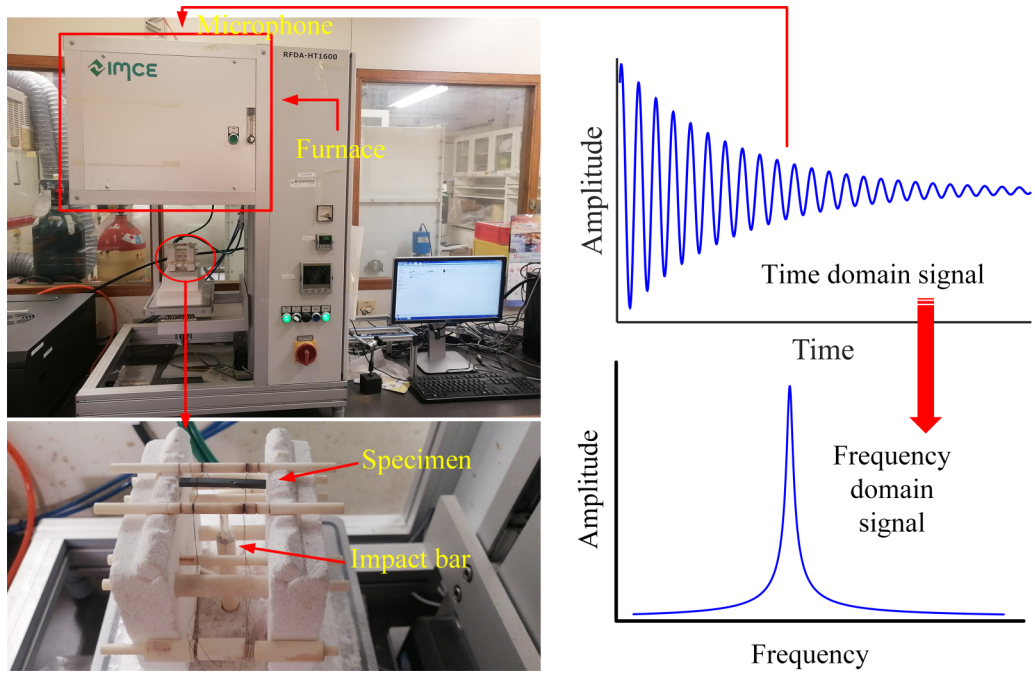

FIG. 1. The specimen, fixture, furnace, and the obtained sound signal in an IET experiment.

III. RESULTS

A. Divergency of the modulus

Figure 2 shows the results of aging at $T_2 = 175\,^{\circ}\mathrm{C}$ after the temperature jumps from $T_1 = T_2 \pm \Delta T$ with $\Delta T = 5$, 10, and 15 °C. An example temperature profile of the two-step aging is shown in the above-left inset, which illustrates the temperature overshoot and slow variations in a jump from $T_1 = 160\,^{\circ}\mathrm{C}$ to $T_2 = 175\,^{\circ}\mathrm{C}$. Though this transition took hundreds of seconds, it is regarded to be a short transient process in comparison with the long aging time at T_1 and T_2 (∼104 s). Also, the relaxation at T_2 starting from $t = 0$ as defined in this inset warrants the measurements of quasiequilibrium relaxation time and Young's modulus.

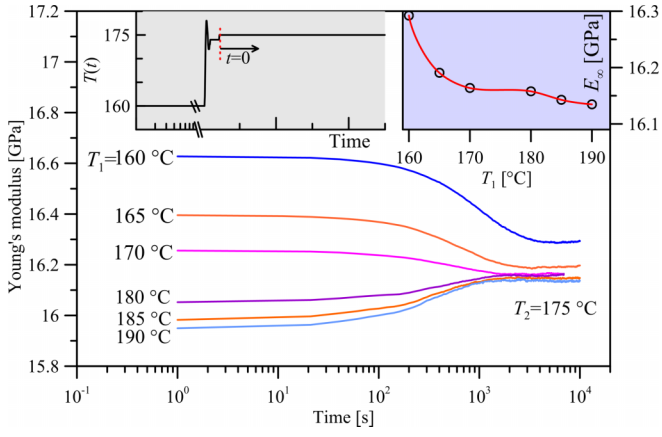

FIG. 2. Two-step aging results of As_2Se_3 glass with $T_2 = 175\,^{\circ}\mathrm{C}$ and $T_1 = T_2 \pm 5$, 10, and 15 °C. Main plot: relaxation and quasiequilibrated Young's modulus at T_2, showing the divergence of Young's modulus relaxation time process, illustrating a T_1 dependence. Above-left inset: a temperature profile from 160 to 175 °C; above-right inset: plot of quasiequilibrium Young's modulus E_∞ against T_1.

As shown in the main plot of Fig. 2, when $\Delta T = 5\,^{\circ}\mathrm{C}$, the relaxation processes after up and down jumps are almost symmetric and the Young's modulus after a long relaxation seemingly merges. With the increase in ΔT, the relaxations after up and down jumps become asymmetric, and more surprisingly, the quasiequilibrium Young's moduli are also different. We averaged the final leveled segment of the Young's modulus data, containing over 400 data points collected in hours, to quantify the quasiequilibrium magnitude of Young's modulus E_∞, as plotted in the above-right inset of Fig. 2 against T_1. Though the difference of E_∞ is small (<1.5%), it is noteworthy that the divergence of E_∞ at T_2 is systematic, i.e., E_∞ decreases with T_1 and up-jump experiments render more deviation than down-jump ones when ΔT is the same.

B. Kovacs' paradox of the relaxation

The normalized modulus change $\delta_E(t) = [E(t) - E_\infty]/E_\infty$ is investigated, as shown in Fig. 3(a) with the fitting curves using a stretched/compressed exponential function:

$$\delta_E(t) = \delta_0 \exp[-(t/\tau)^\beta], \tag{1}$$

where τ is the relaxation time, β is the stretched/compressed exponent, and δ_0 is the scaling constant. As shown in Fig. 3(a), all the relaxation curves are fitted with high quality, and the obtained parameters of τ and β against the initial temperature T_1 are plotted in Figs. 3(b) and 3(c), respectively. It is noted that β is almost unity with the maximum deviation of 0.07. Therefore, it is safe for us to claim that the relaxation $E(t)$ in the chalcogenide glass As_2Se_3 is exponential with negligible stretching and that Kovacs' finding of the diverged relaxation time has been explicitly shown in Fig. 2(b); more specifically,

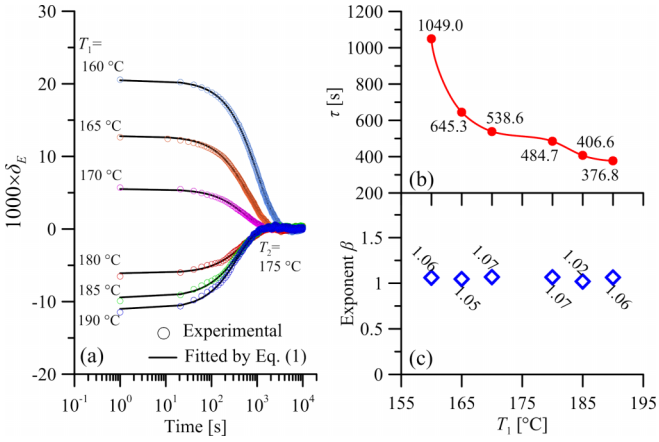

FIG. 3. (a) Plots of the relative change of Young's modulus $\delta_E(t)$ with fitting results using Eq. (1), and plots of (b) relaxation time τ and (c) exponent β against T_1, indicating exponential relaxations.

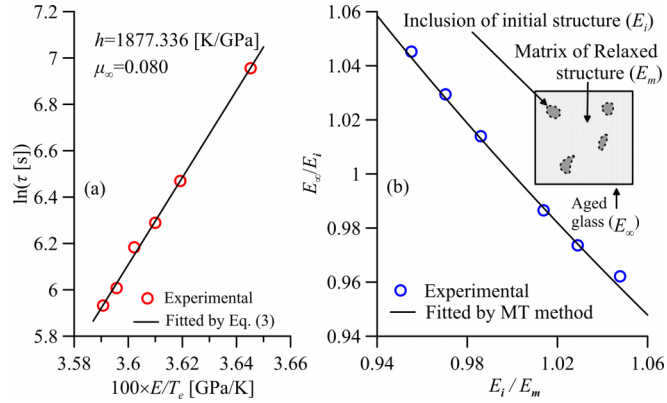

FIG. 4. Analysis of T_1 dependence of (a) relaxation time τ and (b) quasiequilibrium Young's modulus E_∞ based on the elastic model [42] and Mori-Tanaka approach, respectively, with an inset in (b) illustrating the simplification of the T_2-aged glass to be a composite.

τ increases sharply with the decrease of T_1, indicating that going deeper in the initial glass state leads to a slower rearrangement of the microscopic system. This is similar to the simulation result of the hard-sphere system [16].

IV. DISCUSSION

A. History dependence caused by EB

While various models have been proposed to reconcile the conflict between equilibrium dynamics and the history dependence indicated by Kovacs' $\tau_{\rm eff}$ paradox, such as rational thermodynamics [23], stochastics relaxation models [26–28], or the coupling model [41], a loophole in the paradox is indeed the experimental inability to probe the slowest relaxation in a nonexponential process [19,25]. In our experiments, however, the relaxations are exponential, the loophole vanishes, and the history dependence of the relaxation time stands. And we have supplemented with the observation that the long-term relaxation may not bring the system to equilibrium or an ergodic state because E_∞ does not converge, i.e., the ergodicity is broken and the glassy system can only explore a T_1-dependent subregion of the configurational space. This finding echoes the extensive computational and experimental findings that aging a spin system at temperatures below T_g does not bring the system asymptotically to an equilibrium state [4–6]. Note that we cannot exclude the possibility that an ultralong relaxation may bring the system to equilibrium because of the constraint of the experimental system (in our case it is due to the limit of inert gas supply). However, because of all the $E \sim lgt$ curves clearly leveled off as shown in Fig. 2 with durations of the flat segments over 10τ, it is reasonable to claim that the further relaxation, if it exists, needs a time scale well beyond the experimentally accessible range.

We anticipate further a correlation between the dynamics, manifested by τ, and the statics, manifested by E_∞, because the temperature dependencies of them are similar. Based on the elastic model proposed by Mooney [42] which was derived based on Eyring's picture of local molecular movements [43], a relaxation comes about when thermal fluctuations generate a local expansion exceeding a certain critical value. Mooney [42] estimated the probability that these relaxation events were interfered with the thermal longitudinal sound waves and proposed that

$$\tau = \tau_0 \exp\left[\frac{Q}{k_{\rm B}T}\right], \tag{2}$$

where τ_0 is a prefactor, $k_{\rm B}$ is the Boltzmann constant, $Q \propto c_\infty^2 \propto E$ is the activation energy, and c_∞ is the speed of longitudinal sound waves. Note that the temperature T in Eq. (2) is a phonon temperature which does not account for the effect of the nonequilibrium dynamics associated with an unrelaxed atomic configuration [44]. We follow Tools [45] and other researchers [46,47] to involve the effect of structural temperature by introducing an equivalent temperature $T_e \in [T_1,\ T_2]$ to replace T in Eq. (3), because the glass is sufficiently equilibrated at T_1 and then aged at T_2. For simplicity, letting $T_e = \mu T_1 + (1-\mu)T_2$ with $\mu = \mu(t) \in [0,\ 1]$ being time dependent, Eq. (2) is then recast as

$$\ln\tau = \ln\tau_0 + h\frac{E}{T_e}, \tag{3}$$

where $h = Q/(k_B E)$. At a quasiequilibrium state, E_∞ and $\mu_\infty = \mu\ (t \to \infty)$ are constant. Replacing E with E_∞ in Eq. (3), and fitting the results of τ, it is obtained that $\mu_\infty = 0.080$, as shown in Fig. 4, wherein the data points collapse to a straight line given by Eq. (3). The obtained slope $h = 1877.3$ K/GPa, together with $E_\infty = 16.2 \pm 0.1$ GPa (see the above-right inset of Fig. 2), leads to the activation energy of $Q = hEk_{\rm B} = 60.4 \pm 0.4$ kcal/mol, agreeing reasonably well with the activation energy of 68 kcal/mol of As_2Se_3 near T_g [48] determined based on the temperature dependence of shear viscosity.

Though μ_∞ is small, it indicates the nonvanishing structural memory in an aged glass, corresponding to the unmerged E_∞ as shown in Fig. 2(b). We simplify the aged glass to be a composite, wherein the components are the glass patches with different macroscopic physical properties after EB, as sketched in the inset of Fig. 4(b). Denoted by E_i and E_m, the Young's moduli of the subbasins with different macroscopic properties, the ratio E_∞/E_i can be expressed as a function of $x = E_i/E_m$. By neglecting the geometry of the subsystems

TABLE I. Quasiequilibrium Young's modulus at $T_2 = 175\,^{\circ}$C.

T_1 (°C)	E_∞ (GPa)
160	17.04
165	16.70
170	16.42
180	15.90
185	15.61
190	15.33

TABLE II. Quasiequilibrium Young's modulus at differnt T_2.

T_1 (°C)	E_∞ (GPa)	T_2 (°C)	E_∞ (GPa)
160	17.01	170	16.51
180	15.88	170	16.39
163	16.84	173	16.77
183	15.82	173	16.28
167	16.56	177	16.052
187	15.52	177	16.046
170	16.39	180	15.88
190	15.34	180	15.88

with different Young's modulus, i.e., we simply suppose the inclusions are spherical, the effective shear and bulk modulus can be derived based on the Mori-Tanaka (MT) method [49]:

$$G_\infty = G_m + \frac{(G_i - G_m)V_f}{1 + 4(1 - V_f)G_p(G_i - G_r)}$$
$$K_\infty = K_m + \frac{(K_i - K_m)V_f}{1 + 9(1 - V_f)K_p(K_i - K_m)} \tag{4}$$

and

$$G_p = \frac{3(2G_m + K_m)}{10G_m(4G_m + 3K_m)},$$
$$K_p = \frac{1}{3(4G_m + 3K_m)}, \tag{5}$$

where G_∞, G_i, and G_m are the effective shear modulus, shear modulus of initial structures (inclusion), and shear modulus of relaxed structures (matrix), respectively, and K_∞, K_i, and K_m are the corresponding bulk modulus. Then, recall the relations

$$G_\theta = \frac{E_\theta}{2(1 + \nu_\theta)},$$
$$K_\theta = \frac{E_\theta}{3(1 - 2\nu_\theta)}, \tag{6}$$

where E_θ, and ν_θ are Young's modulus and Poison's ratio, respectively; $\theta = i$ and m. Then the effective Young's modulus can be written as

$$E_\infty = \frac{9K_\infty G_\infty}{3K_\infty + G_\infty} = g(E_i, E_r)|_{(\nu_i, \nu_m, V_f)}. \tag{7}$$

That is, E_∞ can be considered as a function of E_i and E_m with parameters of (ν_i, ν_m, V_f). Normalizing Eq. (7) with E_i leads to

$$E_\infty/E_i = y(1, E_m/E_i)|_{(\nu_i, \nu_m, V_f)} = f(x)|_{(\nu_i, \nu_m, V_f)}. \tag{8}$$

With some simple derivations, we obtain

$$\left.\frac{df(x)}{dx}\right|_{(x=1, \nu_i=\nu_m)} + 1 = V_f. \tag{9}$$

The quasiequilibrium Young's moduli (E_∞) at $T_2 = 175\,^{\circ}$C and various T_1 are provided in Table I. To calculate V_f at varied T_2, E_∞ obtained in a series of T_1–T_2 aging experiments are provided in Table II.

Figure 5 shows the modulus-temperature curve of As_2Se_3 glass in the temperature range [40, 150 °C] with the heating rate of 20 °C/min. It leads to the Debye-Grüneisen coefficient of $dE/dT = -0.0071$ GPa/°C.

Interestingly, $f(x)$ leads to V_f because the function is very weakly dependent on ν_i and ν_m. E_m can be determined to be the average of E_∞ of the up and down jumps with $\Delta T = 5\,^{\circ}$C as the two magnitudes are very close. Note that E_i corresponds to the Young's modulus of the quasiequilibrium structures of T_1 quenched to T_2, which can be determined based on the Debye-Grüneisen coefficient. The calculated experimental points of $f(x)$ are plotted in Fig. 4(b) together with the curve predicted by MT theory passing through experimental points when $\nu_i = \nu_m = 0.3$ and $V_f = 0.080\,95$. If ν_i and ν_m vary between [0.1, 0.4], V_f varies between [0.080 94, 0.081 01] based on the best fit of experimental points, exhibiting a very weak dependence on Poisson's ratios. Intriguingly, V_f is identical to μ_∞ though they are determined in completely different ways. This may imply that the quasiequilibrium dynamics and atomic arrangement are closely correlated.

B. Gardner transition point in As_2Se_3

According to Eq. (9), the slope in the plot of Fig. 4(b) near $x = 1$ can be used to estimate V_f. We repeated the aging experiments with $T_2 = 170$, 173, 177, and 180 °C, and $T_1 = T_2 \pm 10\,^{\circ}$C to obtain the relation between V_f and T_2, i.e., the temperature dependence of memory persistence. The results are plotted in Fig. 6. To exemplify, the relaxation curves of $T_2 = 170\,^{\circ}$C and 180 °C are shown in the insets of Fig. 6. It is noted that at 180 °C the two curves merge after a long-time

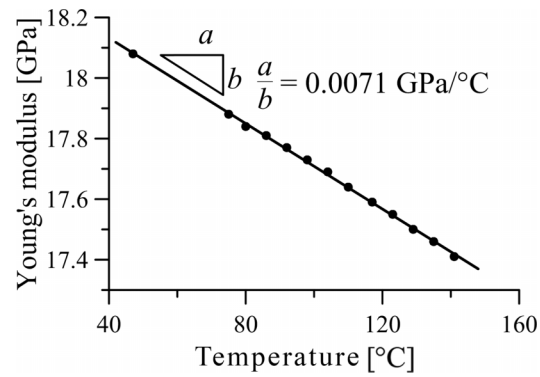

FIG. 5. Temperature dependence of Young's modulus of As_2Se_3 glass. The Debye-Grüneisen is estimated by a linear fit.

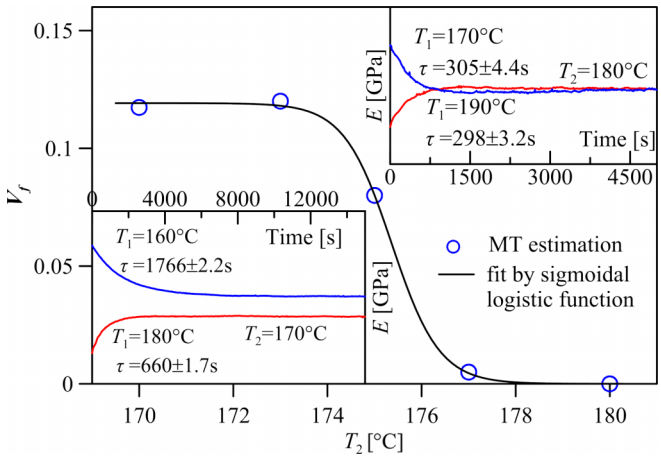

FIG. 6. Plot of the measure of memory persistence V_f against the aging temperature T_2, indicating a clear transition at a critical temperature $T_p \in (177,\ 180\,^{\circ}\mathrm{C})$ with bottom-left and upright insets showing the aging curves $E(t)$ at $T_2 = 180$ and $170\,^{\circ}\mathrm{C}$, respectively, after equilibrated at $T_1 = T_2 \pm 10\,^{\circ}\mathrm{C}$.

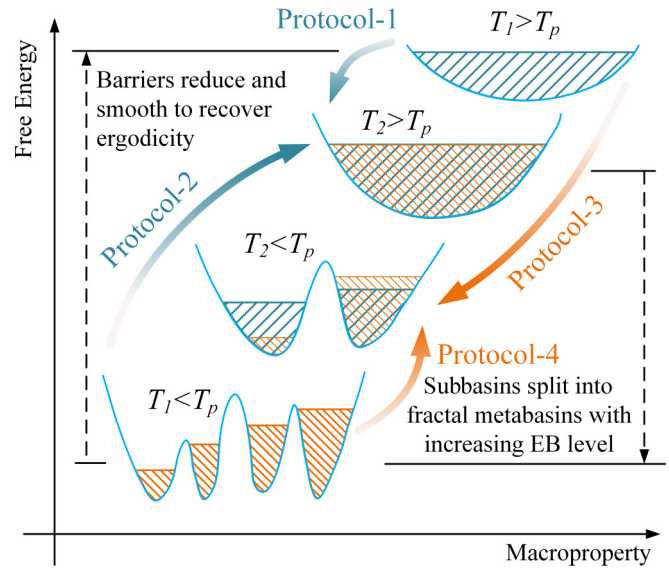

FIG. 7. Variation of the free energy landscape and macrostate distribution in different protocols: when $T_2 > T_p$, the barriers disappear at T_2 that the macroscopic properties of protocol 1 and protocol 2 converges due to the recovery of the ergodicity, even though $T_1 < T_p$; when $T_2 < T_p$, the barriers and fractal metabasins remains and the ergodicity breaks, so that different protocols results in discrepant macrostate distribution as the comprision of protocol 3 and protocol 4, which is the protocol dependence as the Gardner transition displays, even though $T_1 > T_p$.

aging and the exponential relaxation times after up and down jumps are almost identical (∼300 s). Therefore, $V_f = 0$ at $180\,^{\circ}\mathrm{C}$. Noteworthy is that when $T_2 = 177\,^{\circ}\mathrm{C}$, V_f is 0.005 determined from the well separate E_∞ after up and down jumps. Besides, $\tau = 394.0$ and 320.2 s based on exponential fits for up and down jumps at this temperature, respectively, with the expected difference that the up-jump case relaxed slower. Figure 6 suggests there is a critical temperature $T_p \in (177,\ 180\,^{\circ}\mathrm{C})$ initiating an EB, which can be regarded as the Gardner transition point. Below T_p, the structural memory persists, i.e., the system is out of ergodicity; above it, the memory can fade completely, i.e., the system restores ergodicity. For As_2Se_3, T_g is not a uniquely determined temperature but varies in the range 175–180 °C [50] due to the variety of characterization techniques. We hence argue that the critical temperature T_p is within the empirical range of T_g, at least for As_2Se_3, signifying that structural glass transition is not just a slowing-down process. Also, we emphasize that our work has paved the way to uniquely determine T_p through measuring E_∞ after two-step aging with $\Delta T \sim 10\,^{\circ}\mathrm{C}$. The measurement of the exact T_p for As_2Se_3 would only depend on the accuracy and resolution of temperature control and modulus measurement.

Phenomenologically, the persistent memory can be explained based on a rugged free energy landscape [6], namely, a glassy system may be trapped in deep energy basins during aging at T_1, which constrains the exploration of the full energy landscape at T_2 within an experimentally accessible time that is already much longer than the relaxation time estimated from viscosity. This picture is also reminiscent of the "mosaic" transition delineated by the RFOT theory [12], that is, a glassy system transforms into a patchwork consisting of distinguishable atomic arrangements below T_g. In the two-step aging experiments, some patches at T_1 persist at T_2 during the long aging.

Hence, at least for the concerned glass, the physical picture of free energy landscape variation can be schematically shown in Fig. 7. the macroproperties diverge in different protocols when $T_2 < T_p$ even though the T_1 is higher than T_g (protocol 3 and protocol 4), as shown in Fig. 2. The energy barrier is forbidden, and the difference of the energy state at the transition region (T_1) makes the divergent distribution of dynamics after EB, while once $T_2 > T_p$, the barrier reduces and the fractal configuration recedes so that the ergodicity recovers and the system could reach the stable point of the amorphous state even though $T_1 < T_p$ (protocol 1 and protocol 2), as shown in Fig. 6.

However, the mean-field picture based on a free-energy landscape does not explain how a persistent memory forms from the random variations of atomic configurations, especially when $T_p \sim T_g > T_K$ (T_K is the Kauzmann temperature). Therefore, a real-space picture is needed. Trying to establish it, at least with a clue, we note several recent attempts in establishing the connection between static structures and long-time dynamics based on molecular dynamics (MD) simulations. In a very recent investigation of structural-property relation in a binary Lennard-Jones glass, a machine learning algorithm [51] was established, which, after training, can predict long-time dynamics based on the static initial structures. This result is a triumph in decoding the nature of the glass state, as it unveils that the information of initial structures is not "forgotten" in the subsequent relaxation process [52], similar to our results on the initial-state dependence of relaxation time. More transparently, Wang *et al.* [53] conducted MD simulations of $Cu_{50}Zr_{50}$ and found that the activation energy had a strong correlation with the vibrational mean squared displacement (VMSD) instead of the short-range structural indices. As VMSD describes the long-range elastic interactions,

Wang *et al.* [53] argued that the effect of elastic constraint could be the rate-limiting mechanism of structural relaxation in a glass, which is also the reason we employed the elastic model to analyze relaxation time.

Interestingly, Wang *et al.* [53] found that the glass tends to be more heterogeneous during relaxation because the soft spots, those substructures with higher flexibility (higher free energy), tended to flock together, leading to the heterogeneity in both structure and dynamics. Parallelly, Zhang and Lam [54] have established a distinguishable-particle lattice model (DPLM), which can be regarded as an abstraction of soft-spot dynamics. It simplified position randomness in a structural glass to be a random force field between site particles and introduced voids to mimic the motion of soft spots. Such a setup leads to the spatially constrained dynamics (SCD), i.e., only agminated voids bring about significant relaxation events while isolated voids are trapped. The DPLM simulations successfully reproduced the divergence of quasiequilibrium τ_{eff} [55] even though the void concentration and thus the equilibrium state were predefined.

Even though these dynamic models are not established based on the guidance of the Gardner transition theory, their basic ideas could all be encompassed by the multistage fractal configuration of the energy landscape. The memory of the initial state means the relaxation through different basins is frozen, and the soft spots and free volumes are the results of the EB. Encouraged by the DPLM result and MD simulations, we anticipate that a simplified real-space glass model revealing SCD may involve additionally the generation and depletion of soft spots (or voids) that is dependent on the bath as well as structural temperatures, local stress state, and global energy penalty, following those already established in the free-volume picture [56], describing the order of EB and corresponding distribution. Thus, the initial-state dependence, in terms of both relaxation time and quasiequilibrium state, may be revealed as a consequence of the Gardner transition and the associated evolution of the EB.

V. CONCLUSION

The two-step aging experiments with an inorganic glass As_2Se_3 are performed to reveal the clear phenomena of ergodicity breaking based on the measurements of instantaneous Young's modulus. The further fractal of the free-energy landscape within the glass state is reflected through the divergency of the dynamic response at the same temperature with different thermal history. Based on the concept of the Gardner transition, the status of ergodicity breaking and the memory effect are assessed through the theory of classical mechanics. We identified a critical ergodicity-breaking temperature of As_2Se_3 in terms of the volume fraction of the persistent memory, which was within the empirical glass transition range and regarded as the Gardner transition point of As_2Se_3. It should be noted that the two-step aging experiments reveal a higher-order ergodicity-breaking phenomenon of the amorphous system (corresponding to the glass transition, the first-order ergodicity breaking), while if this kind of breaking is infinite dimensional, as in the Gardner transition description, it needs further investigation.

ACKNOWLEDGMENTS

We gratefully acknowledge the finical support of Hong Kong RGC-ECS (Grant No. 25200515) and RGC-GRF (Grant No. 15213619).

H.R. designed the research; J.W. processed the materials preparation; X.W. and J.W. processed the experiment; X.W. and J.W. analyzed and interpreted the data, and X.W., J.W. and H.R. wrote the paper.

[1] A. Cavagna, Phys Rep. **476**, 51 (2009).
[2] T. Castellani and A. Cavagna, J. Stat. Mech. (2005) P05012.
[3] L. Lundgren, P. Nordblad, P. Svedlindh, and O. Beckman, J. Appl. Phys. **57**, 3371 (1985).
[4] H. Mamiya, M. Ohnuma, I. Nakatani, S. Nimori, and T. Furubayashi, Philos. Mag. Lett. **85**, 109 (2005).
[5] M. Bernaschi, A. Billoire, A. Maiorano, G. Parisi, and F. Ricci-Tersenghi, Proc. Natl. Acad. Sci. USA **117**, 17522 (2020).
[6] J.-P. Bouchaud, J. Phys I **2**, 1705 (1992).
[7] L. F. Cugliandolo and J. Kurchan, Phys. Rev. Lett. **71**, 173 (1993).
[8] P. Charbonneau, J. Kurchan, G. Parisi, P. Urbani, and F. Zamponi, Nat. Commun. **5**, 1 (2014).
[9] G. Parisi, Phys. Rev. Lett. **50**, 1946 (1983).
[10] M. Mézard, G. Parisi, and M. A. Virasoro, *Spin Glass Theory and Beyond: An Introduction to the Replica Method and Its Applications* (World Scientific, Singapore, 1987), Vol. 9.
[11] E. Gardner, Nucl. Phys. B **257**, 747 (1985).
[12] G. Biroli and J.-P. Bouchaud, The Random First-Order Transition Theory of Glasses: A Critical Assessment, in *Structural Glasses and Supercooled Liquids*, edited by P.G. Wolynes and V. Lubchenko (Wiley, 2012), Chap. 2, pp. 31–113.
[13] T. R. Kirkpatrick and P. G. Wolynes, Phys. Rev. A **35**, 3072 (1987).
[14] J. Kurchan, G. Parisi, and F. Zamponi, J. Stat. Mech. (2012) P10012.
[15] J. Kurchan, G. Parisi, P. Urbani, and F. Zamponi, J. Phys. Chem. B **117**, 12979 (2013).
[16] Y. Jin and H. Yoshino, Nat. Commun. **8**, 1 (2017).
[17] A. J. Kovacs, in *Fortschritte der Hochpolymeren-forschung* (Springer, Berlin, 1964), p. 394.
[18] G. McKenna, M. Vangel, A. L. Rukhin, S. D. Leigh, B. Lotz, and C. Straupe, Polymer **40**, 5183 (1999).
[19] S. Kolla and S. L. Simon, Polymer **46**, 733 (2005).
[20] C. T. Moynihan, S. N. Crichton, S. M. Opalka, Journal of Non-Crystalline Solids **131**, 420 (1991).
[21] S. Rekhson, Journal of Non-Crystalline Solids **131**, 467 (1991).
[22] C. Moynihan, Vigo, Spain (1997) (private communication).
[23] M. Goldstein and M. Nakonecznyj, Phys. Chem. Glasses **6**, 126 (1965).

[24] J. S. Haggerty, Thermal expansion, heat capacity and structural relaxation measurements in the glass transition region, Ph.D. thesis, Massachusetts Institute of Technology, 1966.
[25] L. Struik, Polymer **38**, 4677 (1997).
[26] M. Parrinello and A. Rahman, J. Chem. Phys. **76**, 2662 (1982).
[27] J. Lutsko, J. Appl. Phys. **64**, 1152 (1988).
[28] S. Franz, M. Mézard, G. Parisi, and L. Peliti, Phys. Rev. Lett. **81**, 1758 (1998).
[29] W. Liu, H. Ruan, and L. Zhang, J. Am. Ceram. Soc. **97**, 3475 (2014).
[30] J. Wang, H. Ruan, X. Wang, and J. Wan, J. Non-Cryst. Solids **500**, 181 (2018).
[31] A. Tverjanovich, Glass Phys. Chem. **29**, 532 (2003).
[32] H.-J. Kim, H. S. Park, Y. Hwang, J.-H. Kim, J.-H. Hong, and K.-S. Lee, Appl. Opt. **49**, 1607 (2010).
[33] T. Zhou, Z. Zhu, X. Liu, Z. Liang, and X. Wang, Micromachines **9**, 337 (2018).
[34] C. A. Angell, Science **267**, 1924 (1995).
[35] Z. Zmrhalova, P. Pilný, R. Svoboda, J. Shánělová, and J. Málek, J. Alloys Compd. **655**, 220 (2016).
[36] *ASTM E1876, Standard Test Method for Dynamic Young's Modulus, Shear Modulus and Poisson's Ratio by Impulse Excitation of Vibration* (ASTM International, West Conshohocken, 2015).
[37] M. Yang, X. Liu, Y. Wu, H. Wang, J. Wang, H. Ruan, and Z. Lu, Scr. Mater. **161**, 62 (2019).
[38] J. Wang, X. Wang, and H. Ruan, J. Non-Cryst. Solids **533**, 119939 119939 (2020).
[39] W. Liu and L. Zhang, Polymers **10**, 1153 (2018).
[40] X. Wang, J. Wan, J. Wang, L. Zhu, and H. Ruan, Mater. Des. **181**, 108071 (2019).
[41] R. Rendell, K. Ngai, and D. Plazek, J. Non·Cryst. Solids **131**, 442 (1991).
[42] M. Mooney, Trans. Soc. Rheol. **1**, 63 (1957).
[43] S. Glasstone, K. J. Laidler, and H. Eyring, *The Theory of Rate Processes* (McGraw-Hill, New York, 1941).
[44] L. F. Cugliandolo, J. Kurchan, and L. Peliti, Phys. Rev. E **55**, 3898 (1997).
[45] A. Q. Tool, J. Am. Ceram. Soc. **29**, 240 (1946).
[46] A. S. Keys, J. P. Garrahan, and D. Chandler, Proc. Natl. Acad. Sci. USA **110**, 4482 (2013).
[47] A. Wisitsorasak and P. G. Wolynes, J. Phys. Chem. B **118**, 7835 (2014).
[48] S. Suzuki, T. Kobayashi, H. Ohno, and S. Kamiya, J. Soc. Mat. Sci. Jpn. **22**, 134 (1973).
[49] G. Shen and G. Hu, *Mechanics of Composite Materials* (Tsinghua University Press, Beijing, 2006), p. 294.
[50] D. W. Henderson and D. G. Ast, J. Non Cryst. Solids **64**, 43 (1984).
[51] V. Bapst, T. Keck, A. Grabska-Barwińska, C. Donner, E.D. Cubuk, S. Schoenholz, A. Obika, A. Nelson, T. Back, and D. Hassabis, Nat. Phys. **16**, 702 (2020).
[52] G. Biroli, Nat Phys. **16**, 373 (2020).
[53] Y. Wang, D. Wei, D. Han, J. Yang, M. Jiang, and L. Dai, Chin. J. Theor. Appl. Mech. **52**, 303 (2020).
[54] L.-H. Zhang and C.-H. Lam, Phys. Rev. B **95**, 184202 (2017).
[55] M. Lulli, C.-S. Lee, H.-Y. Deng, C.-T. Yip, and C.-H. Lam, Phys. Rev. Lett. **124**, 095501 (2020).
[56] D. Turnbull and M. H. Cohen, J. Chem. Phys. **34**, 120 (1961).